

Portland State University

PDXScholar

Physics Faculty Publications and Presentations

Physics

10-1-1971

Comment on Electron Scattering in the Image Potential Well

Pavel Smejtek

Portland State University

M. Silver

Follow this and additional works at: https://pdxscholar.library.pdx.edu/phy_fac



Part of the [Physics Commons](#)

Let us know how access to this document benefits you.

Citation Details

Smejtek, P., & Silver, M. Comment on Electron Scattering in the Image Potential Well. *J. Appl. Phys.* 43, 2451 (1972).

This Article is brought to you for free and open access. It has been accepted for inclusion in Physics Faculty Publications and Presentations by an authorized administrator of PDXScholar. Please contact us if we can make this document more accessible: pdxscholar@pdx.edu.

maximum if one electrode, say at $x=0$, is blocking, since charge compensation by carrier transport in opposite directions is prevented. Integration of Poisson's equation, with $P=0$, gives

$$aD[0, t_0, T(t_0)] = -a \int_0^d [1 - x/d] \rho[x, t_0, T(t_0)] dx < S. \quad (8)$$

In view of Eq. (7) one has $Q = aD$. Therefore, the frozen-in charge, as defined by Eq. (1), is always smaller than the net volume charge.

Q might be vanishingly small. Charge injection and trapping in an isotropic medium having an intrinsic Ohmic conductivity $\sigma(T)$ gives $i = \mu\rho^*E + \sigma E$, where ρ^* is the concentration of free charge and μ is the carrier mobility. If, at one temperature, σ is sufficiently high, $\mu\rho^*/\sigma \ll 1$, $i \approx \sigma E$, and $J \approx 0$ in view of Eqs. (4) and (5). While μ/σ might be independent of T , $\mu\rho^*/\sigma$ is not, since ρ^* depends on detrapping time which is a function of temperature. Therefore, the above inequality might be fulfilled at one temperature but not at some other where one would have $J \neq 0$. Any asymmetry, like heating in a temperature gradient or unequal distribution of

traps, makes σ dependent on x and thus prevents J from becoming zero.

In the absence of retrapping and of macroscopic heterogeneities of structure capable of creating a spatial asymmetry, charge release from a single trapping level produces small external currents because currents to opposite electrodes compensate each other.⁷ Only if carriers have been trapped in asymmetrically filled multiple levels does one record significant charge values in the external circuit. It can also be shown that such a system is not charge invariant.

¹B. Gross and L.F. Denard, *Phys. Rev.* **66**, 26 (1944); C. Bucci and R. Fieschi, *Phys. Rev. Letters* **12**, 16 (1964).

²B. Gross, *J. Electrochem. Soc.* **115**, 376 (1968); *Appl. Opt. Suppl.* **3**, 176 (1969); Northern Electric Co. (Canada) Report No. T0 145, 1970 (unpublished).

³R. Gerson and J.H. Rohrbaugh, *J. Chem. Phys.* **23**, 12 (1955); M.M. Perlman, *J. Appl. Phys.* **42**, 2645 (1971).

⁴J. van Turnhout, *Polymer J.* (Japan) **2**, 173 (1971).

⁵G. Jaffé, *Ann. Physik* **16**, 217 (1933); **16**, 249 (1933).

⁶B. Gross, *An. Acad. Brasil. Ci.* **17**, 219 (1945); H. Kallmann and R. Rosenberg, *Phys. Rev.* **97**, 1596 (1955).

⁷J. Lindmayer, *J. Appl. Phys.* **36**, 196 (1965).

Comment on Electron Scattering in the Image Potential Well*

M. Silver and P. Smejtek

University of North Carolina, Chapel Hill, North Carolina 27514

(Received 22 October 1971)

Comments are made on the model of electron injection into SiO_2 proposed by Berglund and Powell. Their assumptions on electron scattering, disregarding the change of the escape cone with the distance from the emitter, lead to serious underestimation of the injected current. Two alternative models of electron injection, based solely on elastic scattering are discussed and do not predict the experimental results. We suggest that observed field dependence of the injected current into SiO_2 indicates that energy relaxation associated with the injected electrons is responsible for the voltage dependence of the current.

Recently, Berglund and Powell¹ reported on the field dependences of photoinjected carriers into SiO_2 . Experimentally, the current was found to be proportional to $\exp(-x_m/\lambda)$, where $x_m = (e/4\epsilon E)^{1/2}$ is the position of the maximum in the potential due to the image and applied field. In order to explain these results, Berglund and Powell assumed that only those electrons which are emitted within the escape cone at the electrode and which reach the maximum in the potential without momentum exchange scattering, or which remain in this small cone after scattering, can contribute to the current. This assumption which does yield a current proportional to $\exp(-x_m/\lambda)$ is not correct theoretically, because it does not take into account the fact that the escape cone increases rapidly with distance. Consequently, the model seriously underestimates the current. Figure 1 illustrates how the escape cone varies as a function of distance.

An examination of Fig. 1 shows that electrons originally in the small escape cone at $x=0$, if scattered at a distance x away from the electrode, have a reasonably large probability of remaining in the escape cone and, therefore, these electrons are not returned to the cath-

ode. Also, electrons outside the small escape cone at $x=0$, but with enough momentum to reach x , may be scattered into the large escape cone at x . Because of this argument, we conclude that agreement between the Berglund and Powell model and experiment is accidental.

The problem including the change of the escape cone has been treated by Young and Bradbury.² They show that

$$j = j_i \left[1 - \int_0^L \frac{\omega(x) dx}{\lambda \cos \delta} \exp \int_0^x \frac{dx'}{\lambda \cos \delta} \omega(x') \right], \quad (1)$$

where j_i is the injection current from the emitter; the probability of return is

$$\omega(x) = \frac{1}{2} \left[1 - \left(\frac{\varphi(x)}{E_m + \varphi(x)} \right)^{1/2} \right] \text{ for } x \geq x_m,$$

and

$$\omega(x) = \frac{1}{2} \left[1 + \left(\frac{\varphi(x)}{E_m + \varphi(x)} \right)^{1/2} \right] \text{ for } x \leq x_m,$$

where $\varphi(x)$ is the height of the remaining barrier at x , E_m is the excess energy of the electron over the barrier in the absence of an applied field, and δ is the polar angle of scattering.

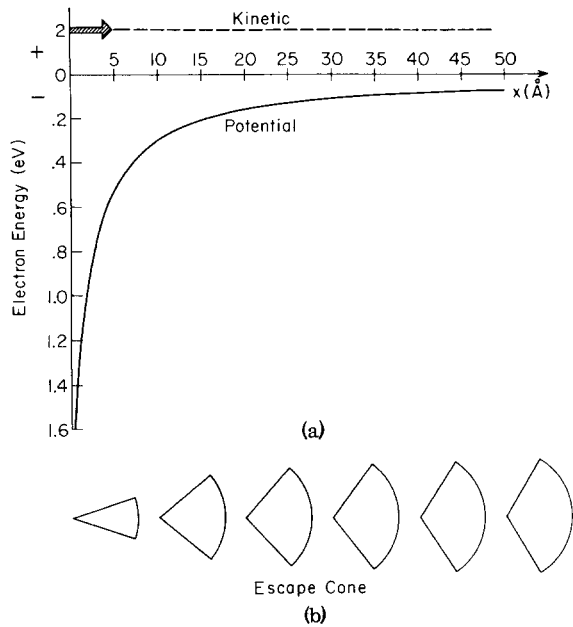


FIG. 1. (a) Energy diagram for electrons injected into image potential well near a metal-insulator surface. (b) The escape cone for electrons having an average energy of +0.2 eV as a function of x for a scattering event at x . The barrier height is 2 eV. Notice how rapidly the escape cone increases with x . An electron scattered, for example, at 20 Å has much greater probability of remaining in the escape cone than an electron scattered at $x=0$.

The Young and Bradbury model which is based on electrons experiencing only momentum exchange scattering is not satisfactory either because it is essentially a single-scattering model. Calculations of the current using the correct image and applied potential in Eq. (1) yield a current practically independent of applied electric field E and λ over a wide range. For example, a current calculated to result from the injection of 1-eV electrons into the medium with $\lambda=100$ Å is about 3% of the injected current for $70 < x_m < 700$ Å.

One might argue that a correction to the Young and Bradbury model might give $j \sim \exp(-x_m/\lambda)$ if one included multiple momentum exchange scattering and no energy relaxation. This calculation has not been tried but should give similar results as a solution to the diffusion equation when the mean free path (MFP) is very small. In order to show the inadequacy of purely diffusive and field-driven motion, for the explanation of the experimental results,¹ we have solved the continuity-of-current equation for a very simple model potential. To make the problem as easy as possible, yet keep the main feature that there is a barrier of finite magnitude and extent, we have chosen the potential shown in Fig. 2. In region 2, we assume a small field so that the concentration of carriers is constant and they have an average kinetic energy of $\frac{3}{2}kT$ at x_m . In this case the current follows the simple Thomson picture,³ and

$$j \approx n(x_m)\mu_2 E_2, \tag{2}$$

where E_2 is the electric field in region 2. To specify the current j , we must solve the continuity-of-current equa-

tion in region 1. In region 1 we assume only momentum exchange scattering, and therefore

$$j = -D(x)\frac{dn}{dx} - n\mu_1(x)E_1; \tag{3}$$

the boundary condition at $x=0$ is

$$j_i = \frac{1}{4}n(0)v(0) + j, \tag{4}$$

where j_i is the injection current from the electrode, $v(0) = [(2/m)(\frac{3}{2}kT + eE_1x_m)]^{1/2}$, and E_1 is the electric field in region 1. The diffusion coefficient and the mobility are functions of x because the kinetic energy is a function of x in region 1, i. e., $D(x) = \frac{1}{3}v(x)\lambda$ and $\mu(x) = e\lambda/mv(x)$, where

$$v(x) = \{(2/m)[\frac{3}{2}kT + eE_1(x_m - x)]\}^{1/2}.$$

Equation (4) can now be solved, yielding

$$\frac{j}{j_i} = \left[1 + \frac{v(0)}{4\mu_2 E_2} \left(\frac{kT + \frac{2}{3}eE_1 x_m}{kT} \right)^{3/2} + \frac{3}{4} \frac{\frac{3}{2}kT + eE_1 x_m}{eE_1 \lambda} \times \left(\frac{kT + \frac{2}{3}eE_1 x_m}{kT} - 1 \right) \right]^{-1}, \tag{5}$$

which is approximately equal to

$$\frac{j}{j_i} \approx \frac{4\mu_2 E_2}{v(0)} \left(\frac{3kT}{2eE_1 x_m} \right)^{3/2}. \tag{6}$$

As is obvious, Eq. (5) does not yield an exponential of the form $\exp(-x_m/\lambda)$ and, therefore, the assumptions regarding the importance of momentum exchange scattering are not justified.

In a similar experiment using hot-electron injection from a tunnel cathode into liquid helium, Silver *et al.*⁴ and Onn and Silver⁵ also experimentally obtained a current proportional to $\exp(-x_m/\lambda)$. They proposed a model involving rapid energy relaxation in the region of x_m . In this case λ is the diffusion length of the hot electrons during their thermalization time and not the MFP for momentum exchange scattering. This model applies at low temperatures or at very short energy relaxation times.

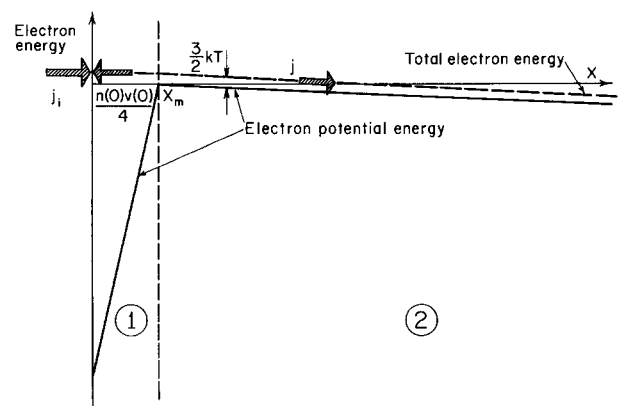


FIG. 2. Energy diagram for electrons injected into a hypothetical potential well near a metal-insulator surface.

We submit that energy relaxation is also a reasonable assumption to explain the experimental results obtained by Berglund and Powell, and therefore they are not deriving the MFP for momentum exchange scattering, but rather a factor proportional to $(\sigma_p \sigma_i)^{-1/2}$, where σ_p is the cross section for momentum exchange scattering and σ_i is the energy relaxation scattering cross section.

We wish to thank Professor Martin Pope of New York University for calling our attention to the paper by Berglund and Powell.

*Work supported by the Army Research Office, Durham, N. C.

¹C. N. Berglund and R. J. Powell, *J. Appl. Phys.* **42**, 573 (1971).

²L. A. Young and N. E. Bradbury, *Phys. Rev.* **43**, 34 (1933).

³J. J. Thomson and G. P. Thomson, *Conduction of Electricity Through Gases* (Cambridge U. P., Cambridge, England, 1928), p. 466.

⁴M. Silver, D. G. Onn, P. Smejtek, and K. Masuda, *Phys. Rev. Letters* **19**, 626 (1967).

⁵D. G. Onn and M. Silver, *Phys. Rev.* **183**, 295 (1969); D. G. Onn and M. Silver, *Phys. Rev. A* **3**, 1773 (1971).

Sputtering of Iron by Fast Neutrons

T. S. Baer and J. N. Anno

University of Cincinnati, Cincinnati, Ohio 45221

(Received 30 August 1971; in final form 13 January 1972)

The atomic sputtering by fast neutrons incident upon a thin iron foil target was determined by measuring the activity of radioactive iron atoms collected during continuous exposure of the target to a fast neutron flux of 4.0×10^{12} neutrons/cm² sec. The sputtering ratio (atoms of iron sputtered per fast neutron crossing the surface of the target) was found to be $(5.7 \pm 0.8) \times 10^{-3}$, assuming an isotropic neutron flux.

This paper reports the measurement of sputtering from the surface of an iron target exposed to fast neutrons. The experimental technique was similar to that used in a previous study of the sputtering from a gold target.¹ The radioactive Fe⁵⁹ atoms produced by the thermal-neutron (n, γ) reaction with Fe⁵⁸ were collected on aluminum-covered quartz plates located near the iron target and, from the measured activity, the sputtering ratio was determined. The apparatus used for the sputtering-ratio determination is sketched in Fig. 1. The overall length of the evacuated quartz tube containing the experimental components was 14 cm. The collector plates, consisting of high-purity Spectrosil quartz with an approximately 500-Å-thick 99.9999% pure aluminum coating, were 5 cm in diameter and 0.16 cm thick. The target was a 3-mil-thick (0.0076-cm) iron foil, with 1 cm² of exposed surface area. The collector plates were spaced 1 cm apart. With this geometry essentially all sputtered atoms are collected.

The quartz tube was evacuated to 10^{-6} Torr and positioned adjacent to the core of the Battelle Research Reactor for a six-day irradiation. The average thermal neutron flux was determined from the activation of the target foil to be $(8.96 \pm 0.50) \times 10^{12}$ neutrons cm² sec. From this measured flux and the known time of exposure (six days), the fraction of the sputtered atoms in the form of Fe⁵⁹ was determined. Aluminum, nickel, and iron cadmium-covered foils (threshold detectors) were used to determine the fast neutron flux. The data were fit to a proton-moderated integral fast neutron spectrum, resulting in a fast flux determination of $(4.0 \pm 0.4) \times 10^{12}$ neutrons/cm² sec above 0.1 MeV. From the measured Fe⁵⁹ activity on the collectors, the fraction of the sputtered atoms in the form of Fe⁵⁹ at the end of irradiation, the counter efficiency, and the decay time between irradiation and counting, the total number of atoms sputtered was determined. The sputtering ratio

Δ was then determined from

$$\Delta = 2N_s / \phi_f S t, \quad (1)$$

where N_s is the number of sputtered atoms, ϕ_f is the fast neutron flux, S is the iron target surface area, and t is the irradiation time. An ordinary polycrystalline iron target was used. Earlier experiments with gold showed only a small effect of target crystallinity on the sputtering ratio.²

After a decay time of approximately five weeks after the irradiation (to allow for the decay of short-lived radioisotopes), the sputtered atoms and the aluminum covering on the two collector plates were removed by washing in a heated 6N HCl bath. Approximately 10 mg of iron carrier was added to the solution from each plate and the iron was precipitated from the solutions by the addition of concentrated ammonium hydroxide. The precipitates were then centrifuged, washed, and slurried into steel planchets for drying. After drying, the planchets containing the sputtered atoms were counted by a Ge-Li detector for 8×10^4 sec each and the resulting spectrum was analyzed to determine the quantity of iron sputtered to the collector plates. The Fe⁵⁹ activity found on the primary collector (the plate opposite the target) was 8.86 ± 0.58 disintegrations/sec as determined by the 1.29-MeV decay γ of Fe⁵⁹ and 7.75 ± 0.45 disintegrations/sec as determined by the 1.10-MeV decay γ of Fe⁵⁹, where the activities have been corrected for the decay time from the end of the irradiation to the time of counting and for counter efficiency. An average of the two values was taken as the iron activity. The Fe⁵⁹ activity found on the secondary collector was 9.36 ± 0.70 disintegrations/sec (1.29-MeV γ) and 9.37 ± 0.55 disintegrations/sec (1.10-MeV γ). The activities of the two plates being nearly equal indicates a sticking fraction for iron on aluminum of approximately 0.5.